

# Non-Covalent Functionalization of Biphenylene Network by Cellulose and Nylon-6: A First-Principles Study

Art Anthony Z. Munio<sup>1,2,\*</sup>, Diamond C. Domato<sup>1</sup>, Alvanh Alem G. Pido<sup>3</sup>,  
Leo Cristobal C. Ambolode II<sup>1,4</sup>

<sup>1</sup> Physics Department, Mindanao State University – Iligan Institute of Technology, A. Bonifacio Avenue, 9200 Iligan City, Philippines; artanthony.munio@g.msuiit.edu.ph (A.A.Z.M.); leocristobal.ambolode@g.msuiit.edu.ph (L.C.C.A.); diamond.domato@g.msuiit.edu.ph (D.C.D.);

<sup>2</sup> College of Arts and Sciences, Jose Rizal Memorial State University, Gov. Guading Adaza Street, 7120 Dapitan City, Zamboanga del Norte, Philippines; artanthonymunio@jrmsu.edu.ph (A.A.Z.M.);

<sup>3</sup> Physics Department, Mindanao State University – Marawi Campus, 9700 Marawi City, Philippines; alvanhalem.pido@msu.edu.ph (A.A.G.P.);

<sup>4</sup> Premier Research Institute for Science and Mathematics (PRISM), Mindanao State University – Iligan Institute of Technology, A. Bonifacio Avenue, 9200 Iligan City, Philippines

\* Correspondence: artanthony.munio@g.msuiit.edu.ph (A.A.Z.M.);

Received: 3.12.2022; Accepted: 5.01.2023; Published: 24.02.2023

**Abstract:** Using first-principles density functional theory, we examined the synergetic interaction and the electronic structure of the newly synthesized biphenylene network functionalized by cellulose and nylon-6. The binding energy of the biphenylene/cellulose and biphenylene/nylon-6 nanocomposite yield a weak bonding state where the adsorption process is exothermic. The interaction is mainly described as physisorption reflected by the binding energy, electron localization function, charge redistribution, and Bader charge transfer analysis. The electronic states of the nanocomposites can be considered a superposition of their constituents, and no evident hybridization of the orbital characters is noticeable. These findings provide a preliminary understanding of polymers' functionalization of the biphenylene network.

**Keywords:** biphenylene network; nylon-6; cellulose; nanocomposite; density functional theory; electronic structure; bonding mechanism; optical properties

© 2023 by the authors. This article is an open-access article distributed under the terms and conditions of the Creative Commons Attribution (CC BY) license (<https://creativecommons.org/licenses/by/4.0/>).

## 1. Introduction

Carbon-based nanostructures have become a worldwide scientific sensation owing to their unique and remarkable properties and promising material for future devices [1,2]. For example, graphene and carbon nanotubes (CNTs) have become the most studied materials owing to their superior thermal, mechanical, and electrical properties over conventional materials [3–6]. Aside from graphene and CNTs, various carbon allotropes such as diamond nano thread, fullerenes, graphenylene, octagraphene, and other forms of carbon are explored for this purpose [7–9]. Although, the main drawback of carbon-based materials is the problem of dispersion which often withholds their applicability [10,11]. Covalent and non-covalent functionalization of these materials is often necessary to overcome the dispersion problem. For instance, the adsorption of oxygen functional groups is used to modify the surface of the graphene to improve its affinity toward the solution [12]. Recently, natural detergents have been used to disperse the SWCNT, leading to a stable near-infrared photoluminescence [13,14]. Non-covalent functionalization of carbon-based nanostructure by polymers is particularly

attractive because one can add new properties while preserving the nature of carbon-based nanomaterials [15]. Covalent functionalization modifies the nanostructure's C-C bonding, thus changing the intrinsic character of the nanomaterial, which often leads to inferior properties (mechanical properties, conductivity, etc.) [12]. The importance of carbon-based nanomaterial is reflected in the number of research and patents in diverse fields, including sensors, electronics, photovoltaic, energy storage, and biomedical technology [3,5,11,16–18].

Recently, a carbon-based nanomaterial (biphenylene network) was successfully synthesized with eight-, six-, and four-carbon rings [19]. This material holds promise, similar to graphene and carbon nanotubes, due to its robust mechanical, superior electrical, and catalytic properties [20,21]. The biphenylene network is ideal for conductive composites, energy storage, and an oxygen-reduction reaction catalyst [20]. However, we anticipate that this material may have a problem in the dispersion due to the van der Waals interactions between networks, as discussed in our previous humble work [22]. Due to the recent discovery by Fan *et al.* [19], computational investigations of the biphenylene network are used to explore its properties and functionalities. First-principles calculation by Luo *et al.* [23] shows that the biphenylene network has robust mechanical properties with an n-type Dirac cone just above the Fermi energy. The simulation also predicted biphenylene's hydrogen evolution reaction performance is better than graphene's. The functionality of the biphenylene network is also recently explored by Gorkan *et al.* [24] using density functional theory. The calculations show that the biphenylene network's physical and chemical properties can be tuned by introducing defects and adsorption of foreign atoms. Furthermore, Al-Jayyousi *et al.* [25] recently convey that the biphenylene network is an impressive anchoring 2D nanomaterial for Li-S batteries. These reports provide a viable strategy for engineering the properties of the biphenylene network to improve existing devices. Despite these scientific reports, there is no investigation into polymers' functionalization of the biphenylene network.

Here, the first-principles density functional theory study was conducted to elucidate the bonding mechanism and the electronic structure of biphenylene/cellulose and biphenylene/nylon-6 nanocomposites. Cellulose and nylon-6 are considered because these materials are widely studied as functional materials of the carbon-based nanostructure. This is mainly due to their remarkable properties and widely established technological applicability, as reflected by the following papers [4,26–31]. The findings reported here indicate that the cellulose biopolymer and nylon-6 are spontaneously adsorbed on the surface of the biphenylene network. This is due to the exothermic nature of the adsorption reflected by the negative binding energy of the nanocomposites. Minimal redistribution of the electrons is observed in the interface, which leads to the conclusion that the cellulose and nylon-6 are adsorbed via physisorption. The main features of the biphenylene network's electronic structure dominate near the Fermi energy of nanocomposites, justifying its weak interaction.

## 2. Materials and Methods

The calculations are conducted using density functional theory (DFT) implemented in the QUANTUM ESPRESSO package, with PBE exchange-correlation functional, PAW pseudopotentials, plane-wave basis set, and Grimme-D3 dispersion correction [32–36]. A 3x3x1 supercell of the biphenylene network is used to model the biphenylene network depicted in Fig. 1a. The energy and charge cutoff energy is set to the standard value, 45 Ry and 330 Ry, respectively. The k-point sampling is set to 5x5x1 centered at the  $\Gamma$  point. In all calculations, a

slab of 15 Å is included to minimize the interaction of the neighboring images. The energy and force threshold is set to 10-8 Ry and 10-5Ry/Bohr, respectively. The electron localization function (ELF), Bader charge analysis, and charge density difference (CDD) of the optimized structures of the nanocomposites are calculated. In the electronic structure calculations, there are 30 k-points considered in calculating band structure in  $\Gamma - X - M - Y - \Gamma - M$  k-path. The density of states is obtained using  $8 \times 8 \times 1$  k-points.

### 3. Results and Discussion

The optimized atomic configurations of biphenylene, cellulose, and nylon-6 are shown in Figure 1a, Figure 1b, and Figure 1c, respectively. First, we benchmark the structural accuracy from other computational reports by measuring the C-C bond of the biphenylene network. The C-C bonds  $l_1$ ,  $l_2$ , and  $l_3$  are measured to be 1.43 Å, 1.44 Å, and 1.41 Å, respectively. These measured bond lengths agree with Luo *et al.* [23] and Hosseini *et al.* [37]. The small variations are attributed to the different approximations utilized in the DFT calculations. It is also noted that this C-C bond is similar to graphene's (~1.42 Å). The molecular model of the cellulose (C<sub>6</sub>H<sub>10</sub>O<sub>5</sub>)<sub>2</sub> (depicted in Figure 1b) is isolated from the bulk form of cellulose I $\beta$  from the paper of Nishiyama *et al.* [38]. The nylon-6 is represented by its monomer (C<sub>6</sub>H<sub>11</sub>NO)<sub>n</sub> displayed in Figure 1c. Periodic boundary conditions are applied such that the biphenylene network, cellulose, and nylon-6 extends to infinity.

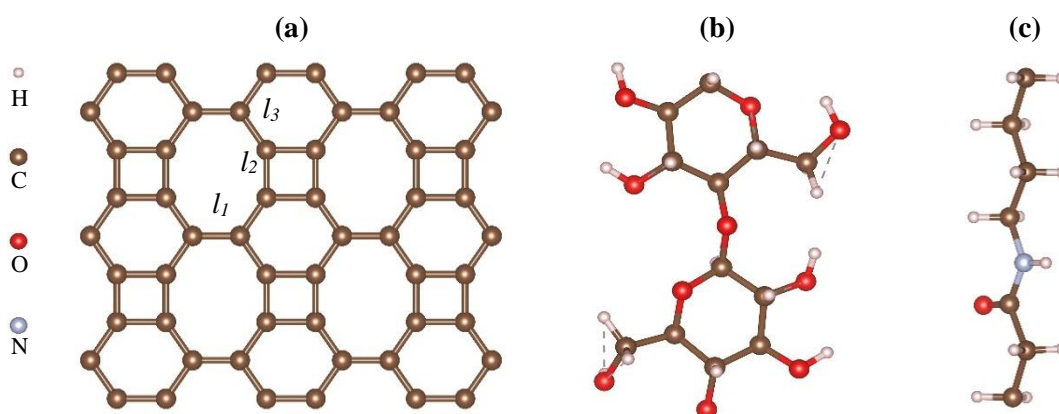


**Figure 1.** The optimized atomic configuration of the (a) 3x31 supercell of biphenylene network, (b) cellulose chain, and (c) nylon-6 unit.

The strength of the interaction is characterized by calculating the binding energy  $E_{\text{binding}}$  using the convention,

$$E_{\text{binding}} = E_{\text{nanohybrid}} - (E_{\text{polymer}} - E_{\text{biphenylene}}). \quad (1)$$

The total energy of the nanohybrid, polymer, and biphenylene network is denoted by  $E_{\text{nanohybrid}}$ ,  $E_{\text{polymer}}$  and  $E_{\text{Biphenylene}}$ , respectively. The binding energy of the nanocomposites in Figure 2a and Figure 2b is -0.86 eV and -0.43 eV, respectively. The binding energy of the biphenylene/cellulose is stronger than biphenylene/nylon-6 nanocomposites two-fold. The difference in the binding energy is attributed to the area of the interface, where a wider area creates a stronger van der Waals interaction [39,40]. The calculated binding energies are similar to the calculated binding energy of GO/cellulose (-0.9 eV), graphene/polymer (-0.34 eV to -0.76 eV), graphene/nylon-6 (-0.52 eV), and SWCNT/nylon-6 (-0.42 eV) [40,41]. Moreover, the equilibrium distance of non-hydrogen atoms of the biphenylene/cellulose and biphenylene/nylon-6 is 3.65 Å and 3.76 Å, respectively. They further indicate the long-range

character of interactions between the constituents of the nanocomposites. The adsorption of the cellulose and nylon-6 bends the biphenylene network locally by  $0.24 \text{ \AA}$  and  $0.015 \text{ \AA}$ , as shown in Figure 2a and Figure 2b. The Bader charge transfer analysis of Figure 3a and Figure 3b indicates a loss of electronic charge of the biphenylene in the nanocomposites with the following value  $0.035 e$  and  $0.006 e$ , respectively. The charge transfer is due to the electron affinity of the atomic oxygen in cellulose and nylon-6. This claim is made clear in Figure 3b, where depletion of the electronic charge (cyan isosurface) is located near the atomic oxygen of nylon-6. The nature of the synergetic interaction of the nanocomposites discussed here is similar to other weakly bonded systems [28,39,40,42,43].

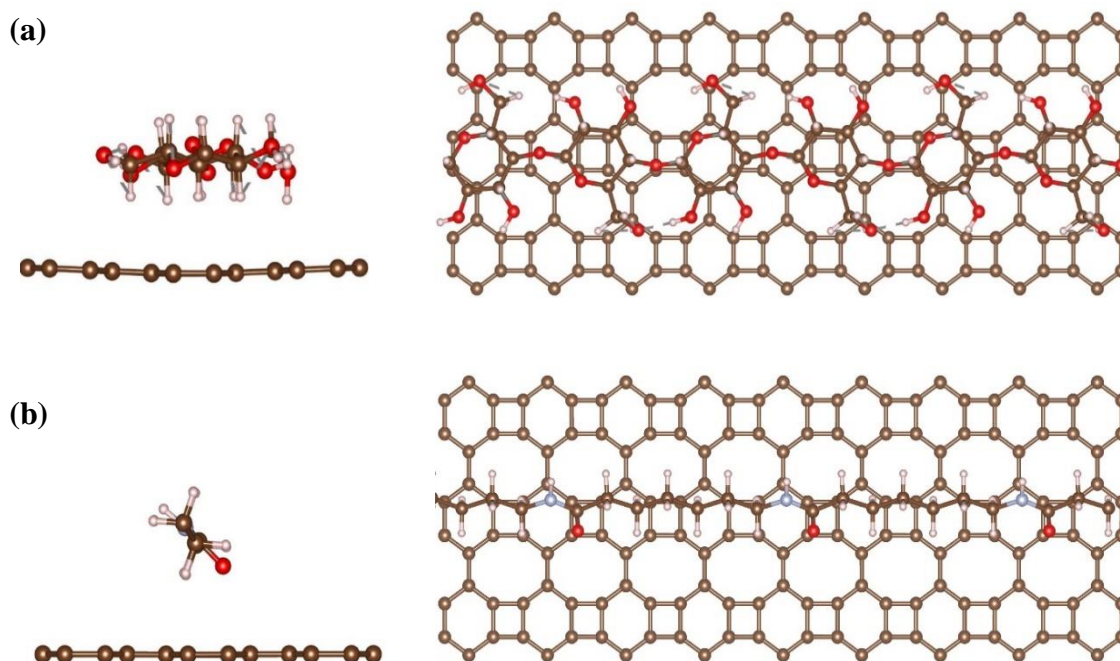


**Figure 2.** The optimized atomic configurations of (a) biphenylene/cellulose and (b) biphenylene/nylon-6 nanocomposites.

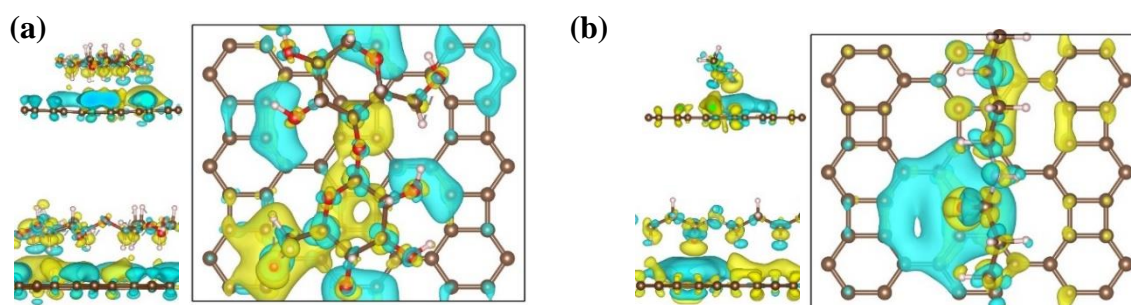


**Figure 3.** The charge density difference of (a) biphenylene/cellulose and (b) biphenylene/nylon-6 nanocomposites. The yellow and cyan isosurface denotes the accumulation and depletion of the electronic charge, respectively.

Further topological analysis of the electronic redistribution was done by calculating the Electron Localization Function (ELF). The ELF describes the nature of the bonding of the systems by analyzing the isosurface and the 2D contour plot of the ELF. The value of the ELF can provide a quantitative description and non-trivial differentiation of chemical interaction [44]. For example, when  $ELF > 0.7$ , this describes a lone pair or covalent bonding (described as yellow-red basins). Meanwhile, when  $0.2 < ELF < 0.7$ , the bonding is similar to metallic bonding or electron-gas (denoted by green-cyan basins).



The isosurface and 2D ELF of the nanocomposites are displayed in Figure 4a and Figure 4b. There is very little ELF value in the interface denoted by the deep blue region, shown in Figure 4a and Figure 4b (right panel). Deformed ELF is also observed at the interface of the nanocomposite, particularly at the hydrogen atom of the cellulose and nylon-6. This is further clarified by calculating the difference between the ELF of the nanocomposites and their isolated constituents (Figure 4c and Figure 4d). The difference in the ELF provides a clear description of the electronic redistribution compared to the CDD in Figure 3a and Figure 3b.

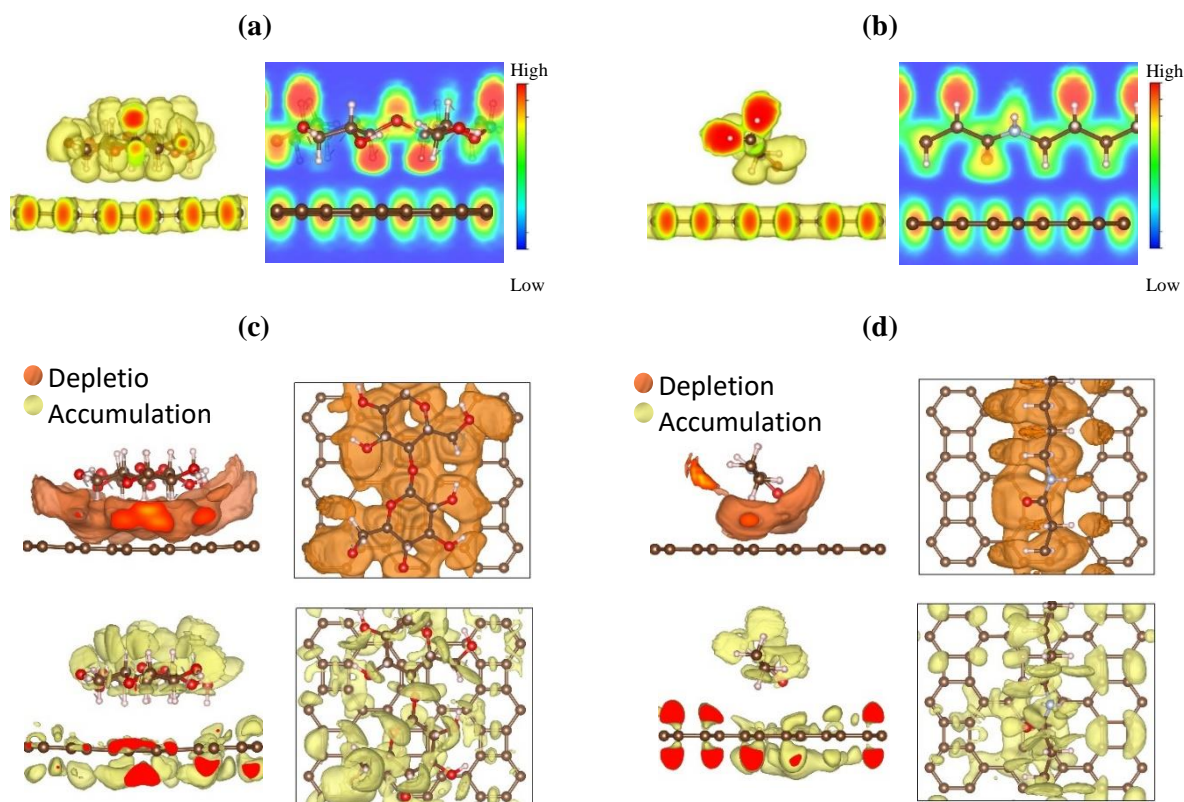


**Figure 4.** The ELF of the (a) biphenylene/cellulose and (b) biphenylene/nylon-6 nanocomposites. (c) and (d) denotes the difference in the ELF of the nanocomposites and their isolated constituents. The isosurface in the depletion and accumulation region is set to 0.02 and 0.0001, respectively.

The electronic band structure of the unit cell and the  $3 \times 3 \times 1$  supercell of the biphenylene network are shown in Figure 5a and Figure 5b. The electronic band of the biphenylene shows multiple bands across the Fermi energy, indicating its metallic nature in agreement with the  $dI/dV$  experiment and computational results [19,24,45]. The n-type Dirac cone is also observed just above the Fermi energy roughly at 0.5 eV, in accord with the report of Luo *et al.*[23]. Figure 5c and Figure 5d display the band structure of biphenylene/cellulose and biphenylene/nylon-6 nanocomposite. The flat bands of the nylon-6 and cellulose states appear roughly at -1.3 eV and 3.3 eV. This indicates that the wide bandgap of the cellulose and nylon-6 is maintained in the nanocomposites. In both cases, the metallicity of the nanocomposites is mainly represented by the biphenylene network.

The DOS of the biphenylene network, cellulose, and nylon-6 is displayed in Figure 6a. The measured bandgap of cellulose and nylon-6 is 4.9 and 4.7 eV, respectively. The calculated bandgap of the cellulose and nylon-6 is in good agreement with the existing reports [46,47]. The flat bands of the cellulose and nylon-6 create sharp peaks in the DOS, proving its insulating properties. The electronic landscape of the biphenylene network in Figure 6a shows states at

the Fermi energy. This result agrees well with the recent experimental and theoretical studies of the biphenylene network [19,23].

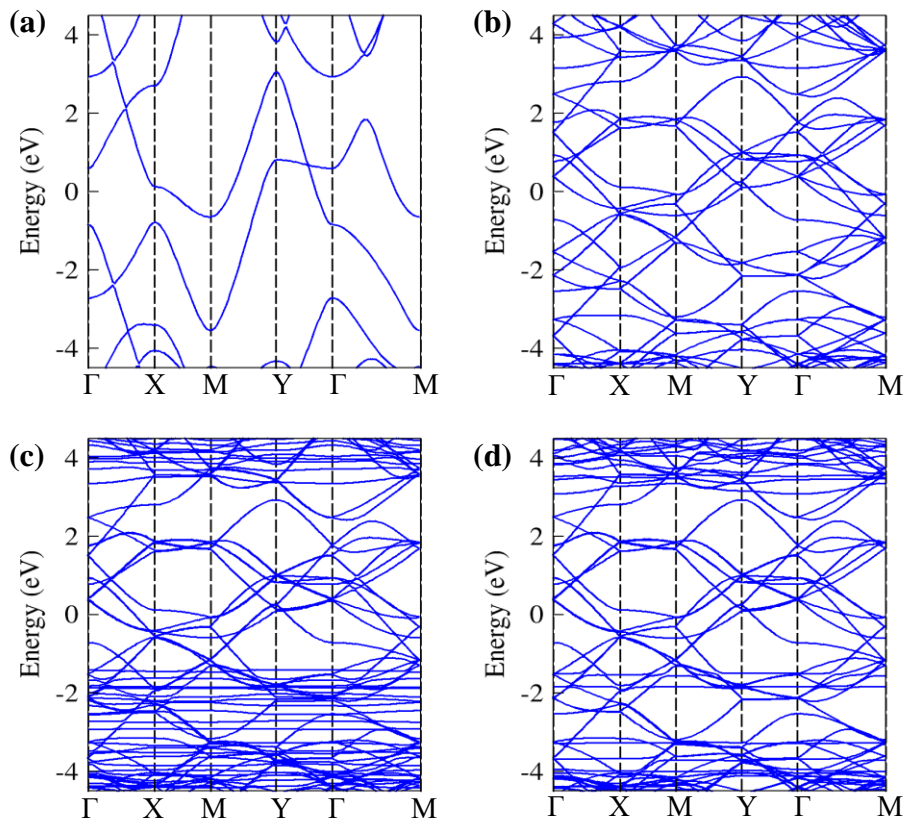


**Figure 5.** The electronic band structure of the (a) unit cell and (b) 3x3x1 supercell of the biphenylene network. (c) and (d) shows the band structure of biphenylene/cellulose and biphenylene/nylon-6 nanocomposites, respectively. The Fermi energy is taken as the reference ( $E_{Fermi} = 0$  eV).

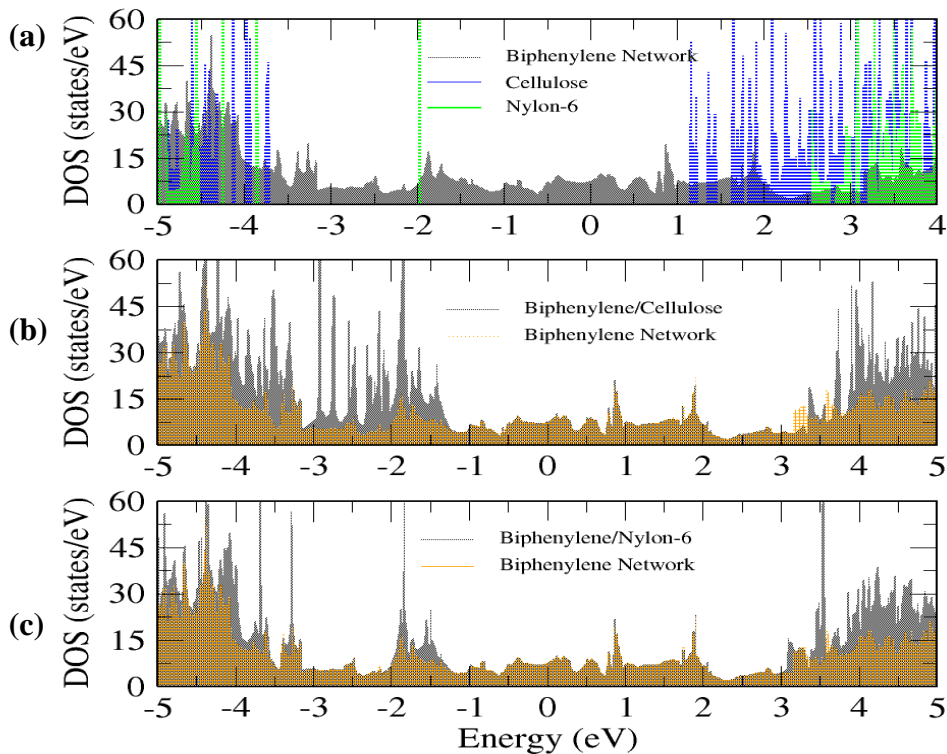


**Figure 6.** The electronic density of states of the (a) constituents, (b) biphenylene/cellulose, and (c) biphenylene/nylon-6 nanocomposite.

The DOS of the nanocomposites is displayed in Figure 5b and Figure 5c. Here, there is no apparent hybridization of the orbital characters between the constituents of the nanocomposites and no broadening of DOS peaks. However, the states of nylon-6 and cellulose appear to have shifted to higher energy relative to the Fermi level. These findings further confirmed the weak interaction between the orbitals of the biphenylene with the adsorbed cellulose and nylon-6. The biphenylene network dominates the DOS of the nanocomposites near the Fermi energy. This is mainly due to the minimal structural deformation of the biphenylene network and negligible charge redistribution. This behavior is similar to graphene/polymer and SWCNT/polymer nanocomposite in which the electronic structures of graphene and SWCNT are well maintained in the polymer composite [39,40].

The results presented provide new insights into the bonding mechanism and electronic structure of the biphenylene network and polymer composite. The weak attachment of the cellulose and nylon-6 on the biphenylene network implies that polymers can be utilized for the non-covalent functionalization of the biphenylene network. Hence, the properties of the biphenylene network and polymers can be combined to fabricate novel and multifunctional such as demonstrated in the following reports of graphene and SWCNT-based polymer composite [5,11,15,48,49]. Although DFT theory has limitations, it is proven to give valuable trends in fundamental chemical interactions and predict the electronic properties of novel materials [9,50,51].

#### **4. Conclusions**

First-principles density functional theory is utilized to give insights into the synergetic interaction and electronic structure of biphenylene/cellulose and biphenylene/nylon-6 nanocomposites. The calculations revealed that the cellulose and nylon-6 can spontaneously physisorbed on the biphenylene network. The nanocomposites' calculated binding energy, electron localization function, and charge transfer analysis support this claim. The synergetic interaction of cellulose on the biphenylene is noted to be stronger than the nylon-6. The difference in the binding energy of the nanocomposites is mainly due to the difference in the interface area, a key feature of physisorption. The electronic DOS of the nanocomposites, particularly near the Fermi energy, resembles that of the biphenylene network. The finding here predicts that the adsorption of the cellulose and nylon-6 gives negligible changes in the biphenylene network's atomic configuration and, therefore, its electronic structure. This study provides a preliminary understanding of the biphenylene network and polymer nanocomposites. The results discussed will serve as a reference for the non-covalent functionalization of the biphenylene network.

#### **Funding**

This study is funded by the Department of Science and Technology Philippine Council for Industry, Energy and Emerging Technology Research and Development (DOST-PCIEERD) through the research project entitled "e-Asia Joint Research Program: Development of Innovative Nanobiodevices Based on Hybrid Materials by Combination of Endemic South Asian Biomolecules and Nanocarbons".

## Acknowledgments

The authors acknowledge the computational resources of the Premier Research Institute of Science and Mathematics (PRISM) at Mindanao State University – Iligan Institute of Technology (MSU-IIT).

## Conflicts of Interest

The authors declare no conflict of interest.

## References

1. Choudhary, N.; Hwang, S.; Choi, W. Carbon Nanomaterials: A Review. In *Handbook of Nanomaterials Properties*; Bhushan, B., Luo, D., Schrickler, S.R., Sigmund, W., Zauscher, S., Eds.; Springer Berlin Heidelberg: Berlin, Heidelberg, 2014; 709–769, [https://link.springer.com/chapter/10.1007/978-3-642-31107-9\\_37](https://link.springer.com/chapter/10.1007/978-3-642-31107-9_37).
2. Anzar, N.; Hasan, R.; Tyagi, M.; Yadav, N.; Narang, J. Carbon Nanotube - A Review on Synthesis, Properties and Plethora of Applications in the Field of Biomedical Science. *Sensors International* **2020**, *1*, 100003, <https://doi.org/10.1016/j.sintl.2020.100003>.
3. Sevilla, M.; Ferrero, G.A.; Fuertes, A.B. Graphene-Cellulose Tissue Composites for High Power Supercapacitors. *Energy Storage Materials* **2016**, *5*, 33–42, <https://doi.org/10.1016/j.ensm.2016.05.008>.
4. Kim, H.C.; Panicker, P.S.; Kim, D.; Adil, S.; Kim, J. High-Strength Cellulose Nanofiber/Graphene Oxide Hybrid Filament Made by Continuous Processing and Its Humidity Monitoring. *Sci Rep* **2021**, *11*, 13611, <https://doi.org/10.1038/s41598-021-93209-5>.
5. Wan, Z.; Chen, C.; Meng, T.; Mojtaba, M.; Teng, Y.; Feng, Q.; Li, D. Multifunctional Wet-Spun Filaments through Robust Nanocellulose Networks Wrapping to Single-Walled Carbon Nanotubes. *ACS Appl. Mater. Interfaces* **2019**, *11*, 42808–42817, <https://doi.org/10.1021/acsami.9b15153>.
6. Abid; Sehrawat, P.; Islam, S.S.; Mishra, P.; Ahmad, S. Reduced Graphene Oxide (RGO) Based Wideband Optical Sensor and the Role of Temperature, Defect States and Quantum Efficiency. *Sci Rep* **2018**, *8*, 3537, <https://doi.org/10.1038/s41598-018-21686-2>.
7. Juhl, S.J.; Wang, T.; Vermilyea, B.; Li, X.; Crespi, V.H.; Badding, J.V.; Alem, N. Local Structure and Bonding of Carbon Nanothreads Probed by High-Resolution Transmission Electron Microscopy. *J. Am. Chem. Soc.* **2019**, *141*, 6937–6945, <https://doi.org/10.1021/jacs.8b13405>.
8. Acquah, S.F.A.; Penkova, A.V.; Markelov, D.A.; Semisalova, A.S.; Leonhardt, B.E.; Magi, J.M. Review—The Beautiful Molecule: 30 Years of C<sub>60</sub> and Its Derivatives. *ECS J. Solid State Sci. Technol.* **2017**, *6*, M3155–M3162, <https://doi.org/10.1149/2.0271706jss>.
9. Kochaev, A.I.; Meftakhutdinov, R.M.; Sibatov, R.T.; Timkaeva, D.A. Optical and Thermoelectric Properties of Graphenylene and Octagraphene Nanotubes from First-Principles Calculations. *Computational Materials Science* **2021**, *186*, 109999, <https://doi.org/10.1016/j.commatsci.2020.109999>.
10. Johnson, D.W.; Dobson, B.P.; Coleman, K.S. A Manufacturing Perspective on Graphene Dispersions. *Current Opinion in Colloid & Interface Science* **2015**, *20*, 367–382, <https://doi.org/10.1016/j.cocis.2015.11.004>.
11. Miyashiro, D.; Hamano, R.; Umemura, K. A Review of Applications Using Mixed Materials of Cellulose, Nanocellulose and Carbon Nanotubes. *Nanomaterials* **2020**, *10*, 186, <https://doi.org/10.3390/nano10020186>.
12. Georgakilas, V.; Otyepka, M.; Bourlinos, A.B.; Chandra, V.; Kim, N.; Kemp, K.C.; Hobza, P.; Zboril, R.; Kim, K.S. Functionalization of Graphene: Covalent and Non-Covalent Approaches, Derivatives and Applications. *Chem. Rev.* **2012**, *112*, 6156–6214, <https://doi.org/10.1021/cr3000412>.
13. Umemura, K.; Hamano, R.; Komatsu, H.; Ikuno, T.; Siswoyo, E. Dispersion of Carbon Nanotubes with "Green" Detergents. *Molecules* **2021**, *26*, 2908, <https://doi.org/10.3390/molecules26102908>.
14. Hirayama, K.; Kitamura, M.; Hamano, R.; Umemura, K. Stable Near-Infrared Photoluminescence of Single-Walled Carbon Nanotubes Dispersed Using a Coconut-Based Natural Detergent. *ACS Omega* **2021**, XXXX, <https://doi.org/10.1021/acsomega.1c04615>.
15. Abreu, B.; Pires, A.S.; Guimarães, A.; Fernandes, R.M.F.; Oliveira, I.S.; Marques, E.F. Polymer/Surfactant Mixtures as Dispersants and Non-Covalent Functionalization Agents of Multiwalled Carbon Nanotubes: Synergism, Morphological Characterization and Molecular Picture. *Journal of Molecular Liquids* **2022**, *347*, 118338, <https://doi.org/10.1016/j.molliq.2021.118338>.
16. Luo, W.; Hayden, J.; Jang, S.-H.; Wang, Y.; Zhang, Y.; Kuang, Y.; Wang, Y.; Zhou, Y.; Rubloff, G.W.; Lin, C.-F.; *et al.* Highly Conductive, Light Weight, Robust, Corrosion-Resistant, Scalable, All-Fiber Based Current Collectors for Aqueous Acidic Batteries. *Advanced Energy Materials* **2018**, *8*, 1702615, <https://doi.org/10.1002/aenm.201702615>.



17. Simões, R.; Neto, V. Graphene Oxide Nanocomposites for Potential Wearable Solar Cells—A Review. *Journal of Materials Research* **2016**, *31*, 1633–1647, <https://doi.org/10.1557/jmr.2016.203>.
18. Egbo, M.K. A Fundamental Review on Composite Materials and Some of Their Applications in Biomedical Engineering. *Journal of King Saud University - Engineering Sciences* **2020**, <https://doi.org/10.1016/j.jksues.2020.07.007>.
19. Fan, Q.; Yan, L.; Tripp, M.W.; Krejčí, O.; Dimosthenous, S.; Kachel, S.R.; Chen, M.; Foster, A.S.; Koert, U.; Liljeroth, P.; *et al.* Biphenylene Network: A Nonbenzenoid Carbon Allotrope. *Science* **2021**, *372*, 852–856, <https://doi.org/10.1126/science.abg4509>.
20. Hudspeth, M.A.; Whitman, B.W.; Barone, V.; Peralta, J.E. Electronic Properties of the Biphenylene Sheet and Its One-Dimensional Derivatives. *ACS Nano* **2010**, *4*, 4565–4570, <https://doi.org/10.1021/nn100758h>.
21. Liu, T.; Jing, Y.; Li, Y. Two-Dimensional Biphenylene: A Graphene Allotrope with Superior Activity toward Electrochemical Oxygen Reduction Reaction. *The Journal of Physical Chemistry Letters* **2021**, <https://doi.org/10.1021/acs.jpcclett.1c03851>.
22. Munio, A.A.Z.; Pido, A.A.G.; Balili, K.I.M. First-Principles Insights On The Bonding Mechanism Of Direct-Stacked Biphenylene Network. *International Engineering Journal For Research & Development* **2022**, *7*, 6–6, <https://doi.org/10.17605/OSF.IO/4FNZ2>.
23. Luo, Y.; Ren, C.; Xu, Y.; Yu, J.; Wang, S.; Sun, M. A First Principles Investigation on the Structural, Mechanical, Electronic, and Catalytic Properties of Biphenylene. *Sci Rep* **2021**, *11*, 1–6, <https://doi.org/10.1038/s41598-021-98261-9>.
24. Gorkan, T.; Çalloğlu, Ş.; Demirci, S.; Aktürk, E.; Ciraci, S. Functional Carbon and Silicon Monolayers in Biphenylene Network. *ACS Appl. Electron. Mater.* **2022**, *4*, 3056–3070, <https://doi.org/10.1021/acsaelm.2c00459>.
25. Al-Jayyousi, H.K.; Sajjad, M.; Liao, K.; Singh, N. Two-Dimensional Biphenylene: A Promising Anchoring Material for Lithium-Sulfur Batteries. *Sci Rep* **2022**, *12*, 4653, <https://doi.org/10.1038/s41598-022-08478-5>.
26. Brakat, A.; Zhu, H. Nanocellulose-Graphene Hybrids: Advanced Functional Materials as Multifunctional Sensing Platform. *Nano-Micro Lett.* **2021**, *13*, 94, <https://doi.org/10.1007/s40820-021-00627-1>.
27. Lv, P.; Feng, Q.; Wang, Q.; Li, G.; Li, D.; Wei, Q. Biosynthesis of Bacterial Cellulose/Carboxylic Multi-Walled Carbon Nanotubes for Enzymatic Biofuel Cell Application. *Materials* **2016**, *9*, 183, <https://doi.org/10.3390/ma9030183>.
28. Shishehbor, M.; Pouranian, M.R. Tuning the Mechanical and Adhesion Properties of Carbon Nanotubes Using Aligned Cellulose Wrap (Cellulose Nanotube): A Molecular Dynamics Study. *Nanomaterials* **2020**, *10*, 154, <https://doi.org/10.3390/nano10010154>.
29. Costa, U.O.; Nascimento, L.F.C.; Garcia, J.M.; Bezerra, W.B.A.; Fabio da Costa, G.F.; Luz, F.S. da; Pinheiro, W.A.; Monteiro, S.N. Mechanical Properties of Composites with Graphene Oxide Functionalization of Either Epoxy Matrix or Curaua Fiber Reinforcement. *Journal of Materials Research and Technology* **2020**, *9*, 13390–13401, <https://doi.org/10.1016/j.jmrt.2020.09.035>.
30. Zhao, Y.; Meng, Y.; Zhu, F.; Su, J.; Han, J. Mechanical Reinforcement in Nylon 6 Nanocomposite Fiber Incorporated with Dopamine Reduced Graphene Oxide. *Materials (Basel)* **2022**, *15*, 5095, <https://doi.org/10.3390/ma15155095>.
31. Fu, S.; Sun, Z.; Huang, P.; Li, Y.; Hu, N. Some Basic Aspects of Polymer Nanocomposites: A Critical Review. *Nano Materials Science* **2019**, *1*, 2–30, <https://doi.org/10.1016/j.nanoms.2019.02.006>.
32. Hohenberg, P.; Kohn, W. Inhomogeneous Electron Gas. *Phys. Rev.* **1964**, *136*, B864–B871, <https://doi.org/10.1103/PhysRev.136.B864>.
33. Giannozzi, P.; Baroni, S.; Bonini, N.; Calandra, M.; Car, R.; Cavazzoni, C.; Ceresoli, D.; Chiarotti, G.L.; Cococcioni, M.; Dabo, I.; *et al.* QUANTUM ESPRESSO: A Modular and Open-Source Software Project for Quantum Simulations of Materials. *J Phys Condens Matter* **2009**, *21*, 395502, <https://doi.org/10.1088/0953-8984/21/39/395502>.
34. Giannozzi, P.; Baseggio, O.; Bonfà, P.; Brunato, D.; Car, R.; Carnimeo, I.; Cavazzoni, C.; de Gironcoli, S.; Delugas, P.; Ferrari Ruffino, F.; *et al.* Quantum ESPRESSO toward the Exascale. *J. Chem. Phys.* **2020**, *152*, 154105, <https://doi.org/10.1063/5.0005082>.
35. Perdew, J.P.; Burke, K.; Ernzerhof, M. Generalized Gradient Approximation Made Simple. *Phys. Rev. Lett.* **1996**, *77*, 3865–3868, <https://doi.org/10.1103/PhysRevLett.77.3865>.
36. Dal Corso, A. Pseudopotentials Periodic Table: From H to Pu. *Computational Materials Science* **2014**, *95*, 337–350, <https://doi.org/10.1016/j.commatsci.2014.07.043>.
37. Hosseini, M.R.; Esfandiarpour, R.; Taghipour, S.; Badalkhani-Khamseh, F. Theoretical Study on the Al-Doped Biphenylene Nanosheets as NO Sensors. *Chemical Physics Letters* **2020**, *754*, 137712, <https://doi.org/10.1016/j.cplett.2020.137712>.
38. Nishiyama, Y.; Sugiyama, J.; Chanzy, H.; Langan, P. Crystal Structure and Hydrogen Bonding System in Cellulose I(Alpha) from Synchrotron X-Ray and Neutron Fiber Diffraction. *J Am Chem Soc* **2003**, *125*, 14300–14306, <https://doi.org/10.1021/ja037055w>.
39. Jelil, J.; Abdurahman, A.; Gülseren, O.; Schwingschlogl, U. Non-Covalent Functionalization of Single Wall Carbon Nanotubes and Graphene by a Conjugated Polymer. *Applied Physics Letters* **2014**, *105*, 013103–013103, <https://doi.org/10.1063/1.4886968>.

40. Jha, S.K.; Roth, M.; Todde, G.; Buchanan, J.P.; Moser, R.D.; Shukla, M.K.; Subramanian, G. Role of Stone-Wales Defects on the Interfacial Interactions among Graphene, Carbon Nanotubes, and Nylon 6: A First-Principles Study. *The Journal of Chemical Physics* **2018**, *149*, 054703, <https://doi.org/10.1063/1.5032081>.
41. Majidi, R.; Taghiyari, H.R. Electronic Properties Of Graphene Oxide In The Presence Of Cellulose Chains: A Density Functional Theory Approach. *Cellulose Chemistry and Technology* **2019**, *53*, 411–416, <https://doi.org/10.35812/CelluloseChemTechnol.2019.53.41>.
42. Gomulya, W.; Gao, J.; Loi, M. Conjugated Polymer-Wrapped Carbon Nanotubes: Physical Properties and Device Applications. *Eur. Phys. J. B* **2013**, *86*, <https://doi.org/10.1140/epjb/e2013-40707-9>.
43. Tran, F.; Laskowski, R.; Blaha, P.; Schwarz, K. Performance on Molecules, Surfaces, and Solids of the Wu-Cohen GGA Exchange-Correlation Energy Functional. *Phys. Rev. B* **2007**, *75*, 115131, <https://doi.org/10.1103/PhysRevB.75.115131>.
44. Koumpouras, K.; Larsson, J.A. Distinguishing between Chemical Bonding and Physical Binding Using Electron Localization Function (ELF). *J. Phys.: Condens. Matter* **2020**, *32*, 315502, <https://doi.org/10.1088/1361-648X/ab7fd8>.
45. Xie, Y.; Chen, L.; Xu, J.; Liu, W. Effective Regulation of the Electronic Properties of a Biphenylene Network by Hydrogenation and Halogenation. *RSC Advances* **2022**, *12*, 20088–20095, <https://doi.org/10.1039/D2RA03673H>.
46. Srivastava, D.; Kuklin, M.S.; Ahopelto, J.; Karttunen, A.J. Electronic Band Structures of Pristine and Chemically Modified Cellulose Allomorphs. *Carbohydrate Polymers* **2020**, *243*, 116440, <https://doi.org/10.1016/j.carbpol.2020.116440>.
47. Sreelatha, K.; Predeep, P. Iodine Doped, Semi-Conducting Nylon 6 Polymers. *Journal of Plastic Film & Sheeting* **2013**, *29*, 127–143, <https://doi.org/10.1177/8756087912464036>.
48. Toraman, G.; Sert, E.; Gulasik, H.; Toffoli, D.; Ustunel, H.; Gurses, E. Polymer Interfaces with Carbon Nanostructures: First Principles Density Functional Theory and Molecular Dynamics Study of Polyetheretherketone Adsorption on Graphene and Nanotubes. *Computational Materials Science* **2021**, *191*, 110320, <https://doi.org/10.1016/j.commatsci.2021.110320>.
49. Rathinavel, S.; Priyadarshini, K.; Panda, D. A Review on Carbon Nanotube: An Overview of Synthesis, Properties, Functionalization, Characterization, and the Application. *Materials Science and Engineering: B* **2021**, *268*, 115095, <https://doi.org/10.1016/j.mseb.2021.115095>.
50. Nasresfahani, S.; Safaiee, R.; Sheikhi, M.H. Application Feasibility of Palladium-Decorated Reduced Graphene Oxide as a CH<sub>4</sub> Gas Nano-Sensor from the Perspective of the van Der Waals Corrected DFT Computations. *Physica E-low-dimensional Systems & Nanostructures* **2021**, <https://doi.org/10.1016/J.PHYSE.2021.114866>.
51. Zhu, B.; Wang, K.; Sun, W.; Fu, Z.; Ahmad, H.; Fan, M.; Gao, H. Revealing the Adsorption Energy and Interface Characteristic of Cellulose-Graphene Oxide Composites by First-Principles Calculations. *Composites Science and Technology* **2022**, *218*, 109209, <https://doi.org/10.1016/j.compscitech.2021.109209>.